

ON THE PROPAGATION OF COSMIC RAYS IN THE GALAXY

JONATHAN ORMES* AND PHYLLIS FREIER

School of Physics and Astronomy, University of Minnesota

Received 1977 July 19; accepted 1977 December 5

ABSTRACT

The details of the leaky-box model for cosmic-ray propagation are presented. The nuclear composition data indicate that the propagation is rigidity dependent. The escape length can be represented by $\lambda_e \propto R^{-0.4 \pm 0.1}$ above 7.6 GV and $\lambda_e = 5.5 \text{ g cm}^{-2}$ below 7.6 GV. From this it follows that the injection spectra of all species must be power laws in total energy or rigidity with $dN/dE \propto E^{-\gamma_0}$ with $\gamma_0 = 2.3 \pm 0.1$. The electron data can also be fitted by using a similar injection spectrum, and both the electron and ^{10}Be data are compatible with a lifetime of $1-2 \times 10^7$ years. The mean density in the storage volume must be $0.15-0.3 \text{ atoms cm}^{-3}$. These data support the assumption that electrons and nuclei have a similar origin within the Galaxy, presumably associated with supernova remnants. Comparison of the lifetime data and the leakage length with radio synchrotron and γ -ray data suggests that the bulk of cosmic rays observed at Earth originate within a 0.5-1 kpc radius around us. Consequences of the model at energies above those currently observed and for the rarer components of the radiation are examined. The model predicts that the spectra of $Z > 30$ nuclei will most closely reflect the source spectrum. If the escape length continues to decrease above 100 GeV per nucleon as $R^{-0.4}$, the asymptotic spectra of primary nuclei will all approach $E^{-2.7}$, the secondary nuclei $E^{-3.1}$, the electron spectrum $E^{-3.3}$, and the positron spectrum $E^{-(3.5-3.7)}$. If the escape length becomes energy-independent, all nuclear spectra will flatten to $E^{-2.3}$ again, whereas the electron spectrum would be unchanged ($E^{-3.3}$).

Subject headings: cosmic rays: abundances — cosmic rays: general — galaxies: structure

I. INTRODUCTION

We examine here in detail the basis for and the consequences of a "leaky-box" model for propagation of cosmic rays in the Galaxy. All the considerable data on the cosmic rays lead to a model which is compatible with what is known about conditions existing in the interstellar medium. The bulk of the cosmic rays can be explained as galactic in nature, with the electrons and nuclei having a common origin. The problem is to determine the containment volume in which the particles diffuse and propagate until, after some mean lifetime, they leak out of the Galaxy. There have been other models recently suggested in which cosmic rays do not leak out of the Galaxy. Rasmussen and Peters (1975) (see also Peters and Westergaard 1977) propose that the Galaxy is closed and that a young nearby component is mixed with the old component. Owens and Jokipii (1977) have suggested a dynamical halo model of cosmic-ray confinement to the Galaxy.

We have developed more fully a model based on the "leaky box" (Cowsik and Wilson 1973; Reames 1974; Ramaty 1974) relating phenomenological aspects of the diffusion and propagation to the physical properties of the interstellar medium. The parameters for the model come from its comparison with data on composition, spectra, change of spectra with energy,

and lifetime of cosmic-ray particles. Such a model must also fit the nonthermal radio emission as well as the γ -ray data. The former acts as a tracer of the electrons and magnetic fields, while the latter traces the cosmic-ray nuclei and matter density in the Galaxy.

Using primarily existing theoretical ideas, we have attempted to find a self-consistent picture of cosmic-ray propagation and to relate it to the large body of existing data. We show that parameters derived by using composition data from the nuclear component can also fit the electron data and that all the data are consistent with a lifetime of $1-2 \times 10^7$ years in the Galaxy. These data are all consistent with a local origin (≤ 1 kpc) for the cosmic rays observed at Earth. The physical properties of the Galaxy implied by this picture are consistent with the γ -ray and radio synchrotron data.

II. BACKGROUND FOR THE MODEL

In this section recent observations which have important consequences for cosmic-ray propagation are outlined. The essential features of a leaky-box model for the storage and propagation of cosmic rays in the Galaxy are described.

a) Cosmic-Ray Sources

While it has long been suggested that cosmic-ray sources were associated with supernova explosions,

* Visiting Professor from NASA Goddard Space Flight Center.

recent work puts this hypothesis on a much more solid observational basis.

Observations of γ -rays produced by the interaction of cosmic-ray nuclei with interstellar matter have shown that there exists a gradient in the galactic cosmic-ray intensity (Puget and Stecker 1974; Stecker 1977; Kniffen *et al.* 1977). In order to explain the γ -ray emissivity, it is found that the cosmic-ray intensity at a galactocentric radius of 5 kpc is probably twice that near the Earth. Other workers have suggested that the spiral structure of the Galaxy is also reflected as a modulation of the cosmic-ray intensity (Kniffen, Fichtel, and Thompson 1977).

These intensity gradients have been associated with the distribution of supernova remnants in the Galaxy (Stecker 1975). It has also been shown that Type II supernova explosions in external galaxies are concentrated in spiral arms. We believe these arguments, while circumstantial, point to the hypothesis that cosmic rays are created in regions of the Galaxy associated with the thin molecular cloud disk (50 pc scale height) in association with supernova events.

Furthermore, recent theoretical work has shown (Scott and Chevalier 1975; Chevalier, Robertson, and Scott 1976) how cosmic-ray electrons might be accelerated in the Cas A supernova remnant; they predict that nuclei would also be accelerated and released with a power-law spectrum in total energy with exponent $\gamma = 2.5$. This mechanism accelerates a mix of supernova ejecta and ambient material to produce the observed composition of cosmic rays (Hainebach, Norman, and Schramm 1976).

On the basis of these arguments, we assume that the cosmic rays are accelerated in supernova remnants and that the galactic gradients are established by the relative frequency of injection events. Higher-resolution studies of the γ -ray intensity may reveal more structure in the cosmic-ray density. However, at the present level of sensitivity, there is no evidence for smaller-scale (≤ 1 kpc) intensity gradients. Electron intensity gradients have been suggested to explain the intensity of the synchrotron radio continuum radiation (Setti and Woltjer 1971; Webber 1976), although alternative explanations in terms of magnetic field fluctuations (Freier, Gilman, and Waddington 1977; Webber 1977) have been advanced.

b) Containment Volume and Diffusion

The particles are injected into the interstellar medium where they are trapped onto magnetic field lines. Their gyroradii are small compared with dimensions of observable structures in the interstellar medium. Therefore their streaming must be essentially along given field lines. If they moved along field lines at velocity $\sim c$, they could go more than 10^3 kpc in their lifetime, so if the particles are to stay near the disk where the matter is, there must be some scattering mechanism which inhibits the particle streaming along the field lines. The very existence of cosmic-ray intensity gradients suggests that the cosmic rays can

travel only at most 1 kpc before diffusing into the halo.

We shall suppose that the scattering mechanism that limits their rapid streaming is due to self-generated waves (Wentzel 1969). If the waves are not damped, they limit the streaming velocity to the Alfvén speed. An original difficulty with this idea was that there were not enough high-energy particles to generate enough waves, thus leading to a strong energy dependence of the effect. This has been overcome with the idea that the waves "cascade" to longer and longer wavelengths so that low-energy cosmic rays generate the waves to inhibit the flow of higher-energy particles (at least up to 100 GeV). (See Skilling 1975; Kulsrud and Cesarsky 1971; McIvor 1977*b*; and review by Wentzel 1974 for details of these arguments.)

We assume then that we are located in a diffusive medium, that the cosmic-ray streaming velocity is limited to the Alfvén velocity (≤ 100 km s⁻¹), and that the cosmic rays we see come from a region of space 0.5–1 kpc around us. Now the particle diffusion is probably controlled by some process similar to that proposed by Lingenfelter, Ramaty, and Fisk (1971), which they labeled compound diffusion. There are two types of diffusion which lead to particle transport. One involves the large-scale motions of field lines in the turbulent gas and the other the motion of particles along those lines. Typical time scales for these phenomena (Parker 1976) must be of the order of 10^7 years; this is the order of the differential rotation time for the Sun to pass through 0.5 kpc. This is also the scale of the spiral structure in the Galaxy, and so 10^7 years is a reasonable large-scale mixing time. The diffusion along the field line is inhibited by waves or perhaps by small-scale (10^{11} – 10^{13} cm) structure in the magnetic field. The large-scale diffusion would be energy-independent; the small-scale scattering must be energy-dependent.

We presume then that the energy dependence of the leakage length is associated with the energy dependence of the wave-scattering diffusion. While this idea is not new (Wentzel 1969), the theoretical explanations are still evolving and are model-dependent (see review by Kulsrud 1975). Higher-energy particles leak out with less scattering.

c) Experimental Basis for Input Parameters

At energies between 50 and 1000 GeV the cosmic-ray proton spectrum measured near Earth is a power law in total energy, $N(E) \propto E^{-2.71 \pm 0.05}$ (Ryan, Ormes, and Balasubrahmanyam 1972). The alpha-particle spectral shape, $E^{-2.74 \pm 0.05}$, is, within errors, the same as the proton spectrum.

Most of the spectral data on the heavier components come from balloon measurements in the energy range 1 GeV per nucleon to 100 GeV per nucleon. In this range several striking features have been found. First, the carbon and oxygen spectra are similar to the proton spectrum (see Balasubrahmanyam and Ormes 1973; Smith *et al.* 1973; Júlíusson 1974; Caldwell 1977). However, the spectra of nuclei such

as Be, B, and N, which are rare at the cosmic-ray sources, appear to be steeper. The difference in spectral exponents, ranging from 0.3 to 0.5 (Smith *et al.* 1973; Júlíusson and Meyer 1973), has been interpreted in terms of an energy-dependent escape mean free path.

The situation with heavier nuclei is less clear. The spectral exponent of iron was initially reported to be in the range 2.2 ± 0.1 (Balasubrahmanyan and Ormes 1973; Júlíusson 1974), while more recent data suggest that it is somewhat steeper, $\gamma = 2.4$ – 2.5 (Orth *et al.* 1978; Caldwell 1977). However, all workers agree that the Fe spectrum is flatter than that of C + O. The issue has been whether this could be explained by the energy dependence of the escape mean free path (Audouze and Cesarsky 1973; Webber *et al.* 1973) or whether some more complex model was required to fit the data (Ramaty, Balasubrahmanyan, and Ormes 1973).

The escape length is determined by using particles whose abundance at the source is presumed to be zero. The collected results of various workers are shown in Figure 1. The data suggest that the escape column density is 5.5 g cm^{-2} at low energy and becomes energy-dependent above 3 GeV per nucleon. This represents physically the point at which the trapping length becomes dependent on the rigidity of particle; however, the trapping time will not be constant but will increase as $1/\beta$ below 3.0 GeV. The trapping, we argue, is a rigidity-dependent phenomenon that is due to the scattering of particles by waves and magnetic inhomogeneities. Therefore, the break occurs at rigidity, $R_0 = 7.6 \text{ GV}$. For electrons this is 7.6 GeV, for protons 6.7 GeV, and for nuclei 3.0 GeV per nucleon. Above 7.6 GV we have fitted

the path length by

$$\lambda_{\text{esc}} = 5.5 \left(\frac{7.6 \text{ GV}}{R} \right)^{0.4} (\text{g/cm}^2)$$

shown in Figure 1.

There have been recent advances in the measurement of cosmic-ray lifetime. *IMP 7* and *8* experiments on abundance of ^{10}Be (Garcia-Munoz, Mason, and Simpson 1975, 1977) at $\sim 100 \text{ MeV}$ per nucleon give a lifetime of 30×10^6 years, but some measurements in the atmosphere at higher energy give lifetimes of 5×10^6 – 10^7 years (Hagen, Fisher, and Ormes 1977; Webber *et al.* 1977); an analysis of the Be/B ratio gives an upper limit of 10^7 years above 1 GeV per nucleon (O'Dell *et al.* 1975). All of the ^{10}Be data are consistent with a lifetime of 1 – 2×10^7 years (at $\beta = 1$).

The lifetime determined from measurements of electron spectra have not yet reached any consensus. New data on the cosmic-ray electrons give steep spectra ($dN/dE \propto E^{-\gamma}$, where $\gamma \approx 3.4$ at high energy) implying that the electrons are also as old as 10^7 years (Hartmann, Müller, and Prince 1977). However, Freier, Gilman, and Waddington (1977), who postulated a high B field to explain the radio emission, calculate a lifetime of 10^6 years based on their data, while Silverberg (1976) determined 3×10^6 years from his data.

For the low-energy cosmic rays to have traversed $5.5 \pm 0.5 \text{ g cm}^{-2}$ of matter in a lifetime of 1 – 2×10^7 years requires that the containment volume have a mean density of 0.15 – $0.30 \text{ atoms cm}^{-3}$, assuming a composition of 90% H and 10% He by number.

We follow Stecker (1977) in describing the local interstellar matter by using three components: (i) a thin region of scale height 50–60 pc containing most of the matter concentrated in cold molecular clouds, (ii) a more diffuse region of atomic hydrogen with a scale height of 100–120 pc, and (iii) a magnetoactive region of scale height 500–600 pc containing magnetic fields and electrons but having very little matter density. The molecular clouds fill 1% of the volume of the thin disk and contain most of the matter; the intercloud medium is of much lower density, 0.1 – 0.2 cm^{-3} . H I is the major constituent locally. The space-averaged total hydrogen density measured locally is 1.1 – $1.3 \text{ atoms cm}^{-3}$ (Spitzer and Jenkins 1975; Burton 1976). If cosmic rays are stored in a volume whose scale height is 0.5–1 kpc, the space-averaged density in that volume will be 0.3 – $0.15 \text{ atoms cm}^{-3}$, which is the density required for a mean particle lifetime of $(1$ – $2) \times 10^7$ years.

From radio surveys we know that the scale height of synchrotron radiation is 0.5–1 kpc (Baldwin 1976). We associate this with the local storage volume of cosmic rays. This scale height is also comparable with the distance the cosmic rays diffuse in the disk. If we assume that the cosmic rays scatter back and forth across the thin sheet of matter, then the 5.5 g cm^{-2} is equivalent to more than 10^3 traversals, even if the particles travel several hundred parsecs in the plane on each traversal. Alfvén waves with short

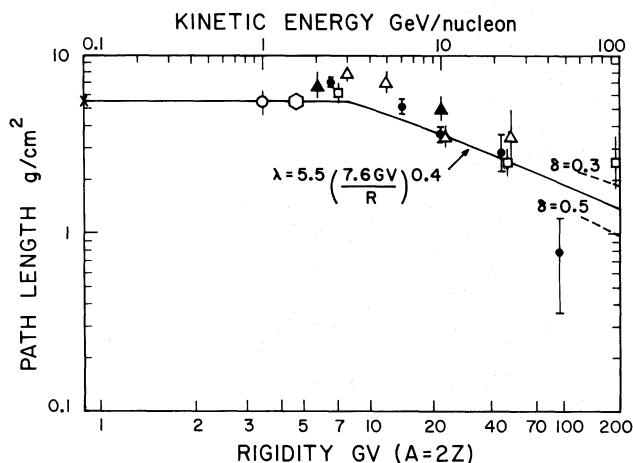


FIG. 1.—Escape path length (derived from ratio of Li + Be + B to C + O) as function of energy and rigidity. Data are from: open circles, Ormes *et al.* (1977); solid circles, Caldwell (1977); crosses, Garcia-Munoz *et al.* (1977); open triangle, Smith *et al.* (1973); square, Júlíusson (1974); closed triangle, Webber, Lezniak, and Kish (1973); hexagon, Shapiro *et al.* (1973).

enough wavelengths to be in resonance with cosmic rays are undoubtedly damped in clouds and probably in most of the thin disk (McIvor 1977a). This may mean that trapping does not occur in the disk, but instead in a region above the disk ($100 \text{ pc} \leq Z \leq 500 \text{ pc}$) where considerable scattering probably can take place (Holmes 1975). In this model, then, we would sit well inside a leaky box whose boundary is slightly transparent in an energy-dependent manner. Each time the wall is hit there is a finite but low probability of transmitting it; this leads naturally to an exponential path length distribution. The waves that scatter cosmic rays may also exist in the hot, low-density portions of the disk itself. However, such a region is well inside the box and has little effect on its configuration or boundaries.

d) Summary of Model

The cosmic-ray data suggest that the particles have passed through an exponential distribution of path lengths with a mean = 5.5 g cm^{-2} . The data are consistent with a path length which is rigidity-independent below 7.6 GV and decreases with increasing rigidity, $\lambda_{\text{esc}} = 5.5 \text{ g cm}^{-2}(7.6/R)^\delta$ where $\delta = 0.4 \pm 0.1$. If we assume that particle intensities are constant in time and can be described by a steady-state "leaky-box" diffusion model, then it follows from the data that the particles are injected into the interstellar medium with spectra $dN/dE \propto E^{-\gamma_0}$ with $\gamma_0 = 2.3 \pm 0.1$. We assume that the injection spectra are power laws in total energy per nucleon, but power laws in rigidity would fit just as well. Implicit in this model is the assumption that all cosmic-ray components (electrons, protons, He, C, O, Ne, Mg, Si, Fe, and traces of other nuclei) are accelerated in the Galaxy.

We shall show that this model, which follows from the data on nuclear composition, also fits the electron data and is consistent with what is known about matter distribution in the interstellar medium, as well as the radio synchrotron and γ -ray data.

III. COMPARISON OF MODEL WITH DATA

a) The Nuclear Component

In the equilibrium steady-state model, the intensity J_i of particles of type i can be written

$$\frac{\partial J_i}{\partial t} = Q_i + \sum_{j>i} \frac{J_j}{\beta\tau_{ji}} - \frac{J_i}{\beta\tau_e} - \frac{J_i}{\beta\tau_{\text{int}}} - \frac{J_i}{\tau_{\text{decay}}}, \tag{1}$$

where Q_i is the source term, the next term is due to spallation of particles of type j into type i with a mean time τ_{ji} , and the last terms are due to escape, interactions, and radioactive decay, where appropriate. The terms $\beta\tau$ represent times to get from interaction to interaction. The time coordinate can be transformed to a column density by $X = m_p \bar{n} \beta c t$, \bar{n} being the average interstellar hydrogen density. In this model clouds and other structures in the Galaxy are crossed

a large number of times, so we are justified in using the average density. We assume that a steady-state situation exists in which $\partial J_i / \partial t = 0$ for all species, and so for stable nuclei we have

$$J_i \left(\frac{1}{\lambda_{\text{esc}}} + \frac{1}{\lambda_{\text{int}}} \right) = \frac{Q_i}{nm_p c} + \sum_{j>i} \frac{J_j}{\lambda_{ji}}, \tag{2}$$

where λ_{esc} is the escape mean free path, λ_{int} is the interaction mean free path for type i , and λ_{ji} is the interaction mean free path for type j to go into type i . We assume there are no energy losses during the propagation other than ionization energy loss which we have neglected. The Earth is possibly located inside an expanding region; however, the expansion velocity is only a few km s^{-1} (Lindblad *et al.* 1973), so diffusing into this region should not involve significant energy loss.

Using the rigidity-dependent escape, we can define an effective mean free path

$$\frac{1}{\lambda_{\text{eff}}} = \frac{1}{\lambda_{\text{esc}}} + \frac{1}{\lambda_{\text{int}}} \tag{3}$$

as a function of rigidity for each species

$$\lambda_{\text{eff}} = \left(\frac{1}{5.5 \text{ g cm}^{-2}(7.6 \text{ GV}/R)^\delta} + \frac{1}{\lambda_{\text{int}}} \right)^{-1}. \tag{4}$$

Below 7.6 GV $\delta = 0$, and λ_{eff} is rigidity-independent. Above 7.6 GV, $\delta = 0.4 \pm 0.1$. The λ_{int} we have used are given in Table 1 for an interstellar medium which is 90% H and 10% He. The λ_{eff} are shown in Figure 2 for protons, carbon, and iron. For nuclei which are present at the sources and for which

$$\frac{Q_i}{nm_p c} \gg \sum_{j>i} \frac{J_j}{\lambda_{ji}},$$

e.g., H, He, C, O, and Fe, we can neglect the secondary component and compute approximate spectra

$$J_i \propto \lambda_{\text{eff}} Q_i,$$

TABLE 1
INTERACTION LENGTHS IN INTERSTELLAR MEDIUM

Nucleus	$\lambda_{\text{interaction}}^*$ (g cm^{-2})
H.....	33.5
He.....	13.2
Li.....	11.8
B.....	8.2
C.....	7.6
O.....	6.2
Ne.....	5.3
Si.....	4.2
Fe.....	2.6

* The interstellar medium is 90% H, 10% He by number of atoms.

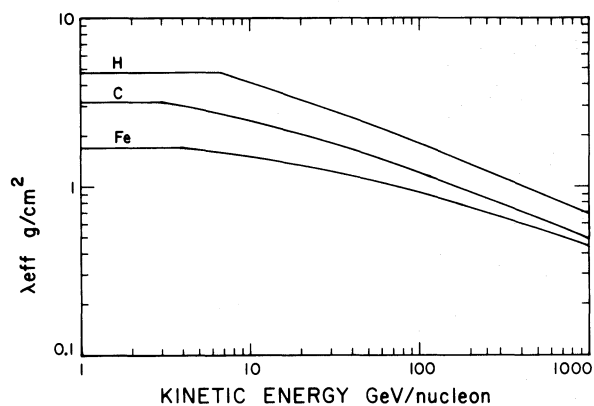


FIG. 2.—The effective mean free path (including interactions and escape) for protons, carbon, and iron as a function of energy per nucleon.

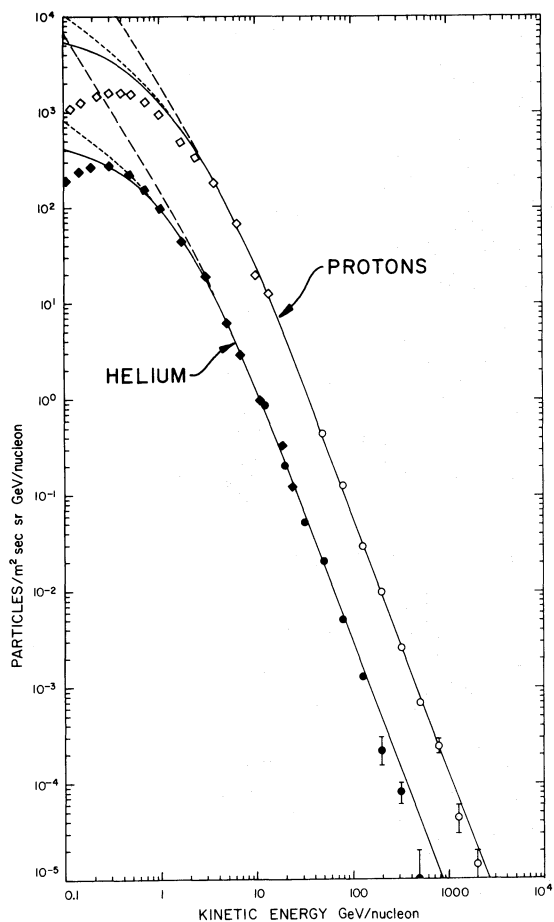


FIG. 3.—Differential intensities of protons and helium. *Solid lines*, fit to an input spectrum, $E^{-2.3}$, with the rigidity-dependent escape: *open symbols*, protons; *solid symbols*, helium. *Circles*, Ryan *et al.* (1972); *diamond at $E > 1$ GeV*, Ormes and Webber (1965); *diamonds at $E < 1$ GeV*, Lezniak and Webber (1971). Fermi input spectra, *dotted line*; power laws in rigidity, *dashed line*, are also shown (see § IVc).

where

$$Q_i \propto \frac{dN_i}{dE} \propto E^{-\gamma_0} (E = \text{total energy per nucleon}).$$

If the source spectrum has slope γ_0 , then the observed spectra will all have slope $\gamma_0 + \delta$ at the highest energies. Since for protons $\lambda_{\text{esc}} \ll \lambda_{\text{int}} = 33.5 \text{ g cm}^{-2}$, the protons reach their asymptotic spectra at quite low energy. The fit to the proton and helium data from Ryan, Ormes, and Balasubrahmanyam (1972) is shown in Figure 3. The data are an excellent fit to power law in total energy from 5 GeV to 1000 GeV. Below 5 GV in rigidity the intensities are reduced by solar modulation.

The injection spectra for the secondary nuclei Li, Be, and B have exponents $\gamma_0 + \delta$, as they are produced mainly by the equilibrium spectra for the C and O nuclei. The Li, Be, and B nuclei can also escape, further steepening their spectra. At high energies the secondary nuclei should have exponents $\gamma_0 + 2\delta$. Data on boron are the most statistically significant and are the least affected by atmospheric background. These data are shown in Figure 4. The differences in

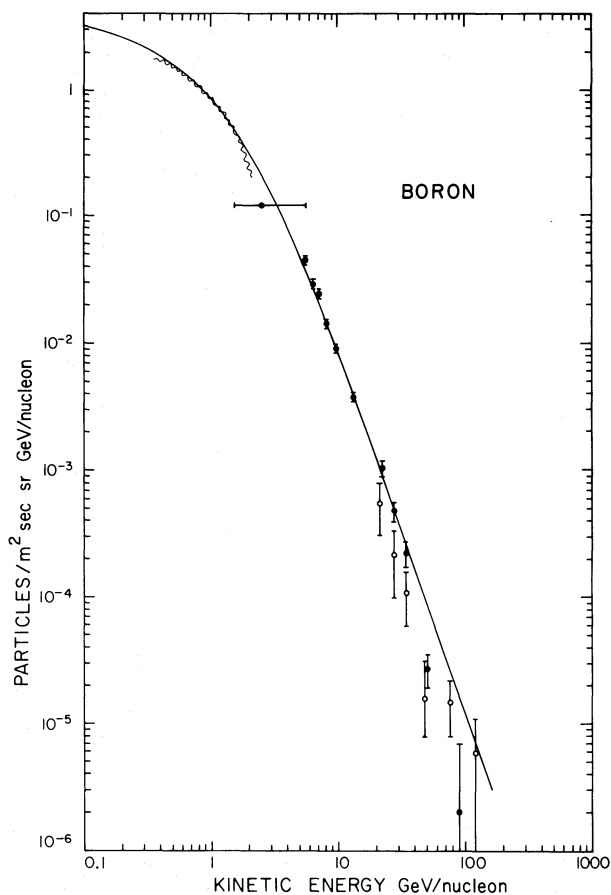


FIG. 4.—Fit of model to boron data. *Open circles*, Jüliusson (1974); *wiggly line*, Maehl *et al.* (1977); *closed circles*, Caldwell (1977).

intensity between Caldwell (1977) and Júliusson (1974) can be traced to differences in atmospheric corrections. We believe it is important to carry out further measurements of these secondary nuclei between 1 and 100 GeV per nucleon above the atmosphere.

In Figures 5 and 6 we compare the model with iron and oxygen data. Because the interaction length of iron is only 2.6 g cm^{-2} , interaction losses at low energy are more important than escape losses, so the spectrum of iron is closer to the injection spectrum and will be flatter. To first order, the model is insensitive to changes in δ of ± 0.1 provided that $\gamma = \gamma_0 + \delta = 2.7$, which is the best known parameter. In second order, reducing δ makes the flatter iron spectrum extend to higher energies, and vice versa.

For oxygen, we have compared the model at high energies with the extensive data of Júliusson (1974) and Caldwell (1977). The C + O data of Balasubrahmanyan and Ormes (1973) are $\sim 2\sigma$ steeper than predicted by this model. It was this spectrum which was so much steeper than their iron data that led to the suggestion (Ramaty, Balasubrahmanyan, and Ormes 1973) that iron was due to a separate source. There is

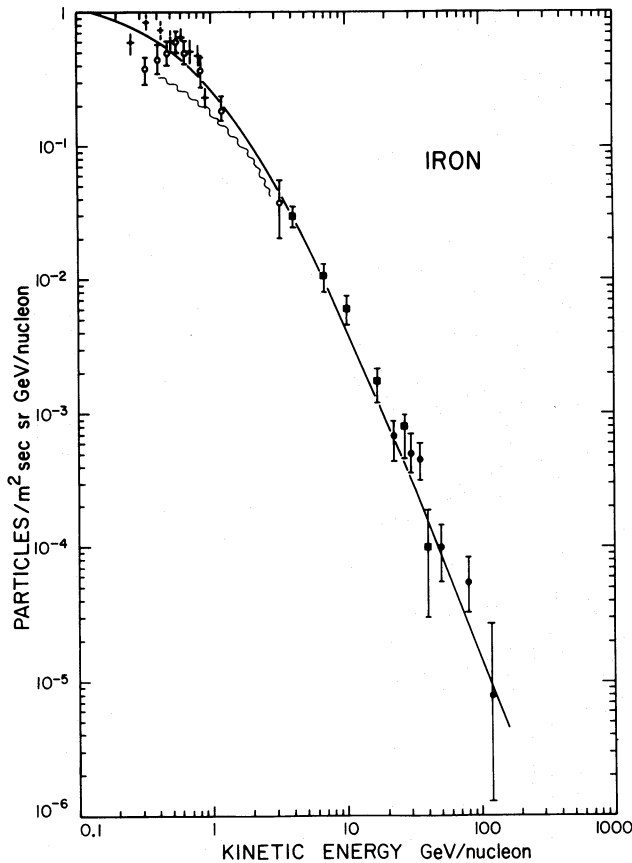


FIG. 5.—Fit of model to iron data. Closed circle, Júliusson (1974); solid square, Ormes and Balasubrahmanyan (1973); open circle, Webber and Ormes (1967); cross, Freier and Waddington (1968); wiggly line, Maehl *et al.* (1977).

reason to doubt the C + O data on which this conclusion was reached. As first noted by Webber (1973), their intensity of C + O was about a factor of 2 lower than that of other workers. This, of course, affected the Fe/C + O ratio, making the energy dependence too extreme when compared with that of other workers at lower energy. Orth *et al.* (1978) and Caldwell (1977) have recently determined both the Fe and C + O spectra, and both claim that their data can be explained by a steady-state leaky-box model such as the one being discussed in this paper.

b) The Electrons

Although there are still discrepancies in the measurements of the local intensity of electrons greater than 5 GeV, they agree to about a factor of 4. We shall determine whether this model can reconcile these electron intensity measurements with the nonthermal radio emission. We shall also see that the electron spectrum is consistent with an electron lifetime equal to the lifetime of the nuclear component.

i) Radio Emission

Synchrotron emission, the principal component of the galactic nonthermal radio emission, is proportional to the number density of electrons, their energy spectrum, and the magnetic field energy density integrated along the line of sight. In order to determine the electron intensity corresponding to the average radio emission, we use the relationship between electron spectrum and synchrotron radiation (Shklovskii 1960)

$$I_\nu = 1.3 \times 10^{-22} (2.8 \times 10^8 c)^{(\gamma-1)/2} \times \mu(\gamma) K B^{(\gamma+1)/2} L_\nu^{-(\gamma-1)/2} \text{ ergs cm}^{-2} \text{ s}^{-1} \text{ sr}^{-1}, \quad (5)$$

where L is the line-of-sight distance, and the differential energy spectrum of electrons is of the form

$$N(E)dE = KE^{-\gamma}dE, \quad (6)$$

with K in ergs cm^{-3} . The function $\mu(\gamma)$ has been evaluated by Shklovskii. The function $\mu(2.9) = 0.090$, and $\mu(\gamma)$ does not vary significantly for $\gamma = 2.8-3.2$. At high frequencies the radio spectrum, $\nu^{-\alpha}$, with $\alpha = 0.95$, corresponds to an electron spectrum with $\gamma = 2\alpha + 1 = 2.9$.

There have been many studies of the relationship of the locally measured electron intensity to the nonthermal radio emission in the Galaxy. (For a summary see Daniel and Stephens 1975; Ginzburg and Ptuskin 1976.) At energies below 5 GeV the radio emission has been used to predict the electron intensity and thus deduce the amount of solar modulation. Typically there have been uncertainties or discrepancies between the electron spectrum predicted from radio measurements and that measured locally, corrected for modulation, on the order of 4-10. As has been

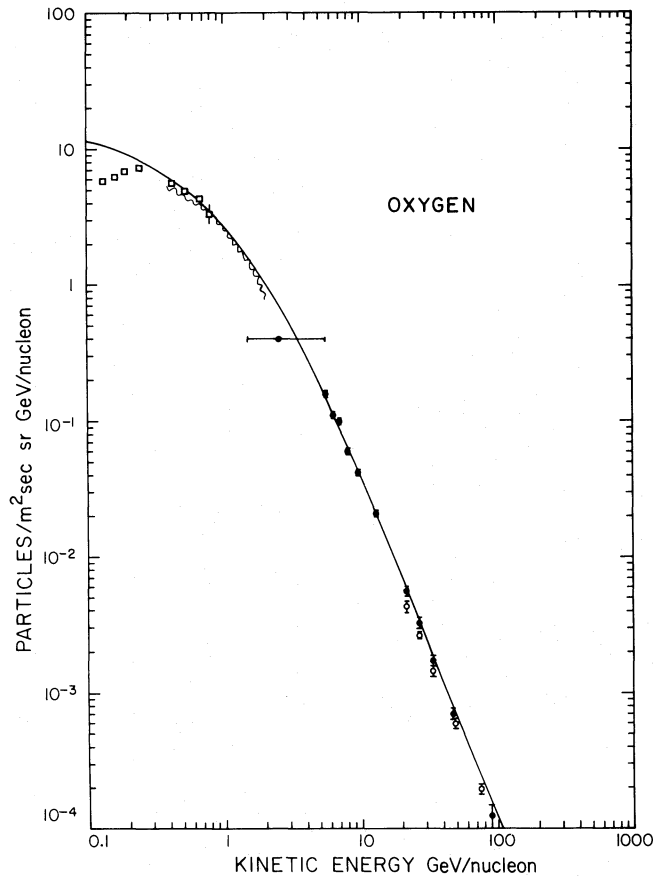


FIG. 6.—Fit of model to oxygen data. *Open circle*, Jüliusson (1974); *closed circle*, Caldwell 1977; *open square*, Wefel *et al.* (1977); *wiggly line*, Maehl *et al.* (1977).

noted recently (Freier, Gilman, and Waddington 1977; Webber 1976, Badhwar, Daniel, and Stephens 1977), even at higher electron energies, where solar modulation effects are negligible, there remains a discrepancy between locally measured electron intensities and those deduced from the nonthermal radio measurements. Possible reasons suggested for this discrepancy have been the effect of clumpy magnetic fields, spatial variation of electron intensity, and higher values for the mean galactic magnetic field than those measured by Faraday rotation.

Figure 7 shows average radio spectra measured in four different directions as summarized by Daniel and Stephens (1975). Data from the whole sky survey at 150 MHz of Landecker and Wielebinski (1970), from the high-resolution surveys at 408 MHz (Green 1974), and from surveys at frequencies up to 15.5 GHz (Hirabayashi 1974) have also been included. The highest intensity is obtained toward the center; the intensity in the anticenter direction is down by a factor of about 5–10, and the intensity in the halo direction is decreased by another factor of 2. None of the plotted data are directly from the galactic center, where the intensity is a factor of 2 higher.

Surveys with high resolution (e.g., 3' of Green

1974) show many individual sources along the galactic plane. These are H II regions as well as SN remnants. The brightness temperature for the continuum background, with sources excluded, has been averaged by Green over strips $\pm 3^\circ$ in latitude and plotted as a longitude distribution. Even excluding sources, he has observed variations of a factor of 2 or 3 in different directions toward the galactic center. At high frequencies, Hirabayashi (1974) has combined his measurements at 4.2 and 15.5 GHz with other measurements of equivalent angular resolution ($\sim 10'$) at other frequencies to resolve the thermal and nonthermal components of the radiation. For six points along the galactic equator selected to be free of H II regions, he found a temperature spectral index of the nonthermal component of -2.9 to -3.0 . A typical spectrum corresponding to a mean temperature spectral index of -2.95 and a mean brightness temperature of 3.7 K at 2 GHz is plotted in Figure 7 for $b = 0$, $l = 26 \pm 6^\circ$. Even though Hirabayashi chose directions free from H II regions, he also found brightness temperatures varying by factors of 2–3 in different directions. These radio observations support the evidence that there are intensity variations throughout the Galaxy of the order of 2–3.

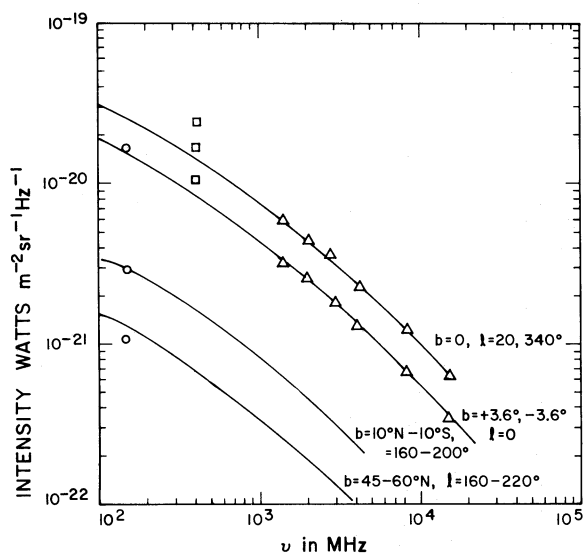


FIG. 7.—Radio spectra taken in four different directions. The upper two curves are from general direction of galactic center but removed in longitude (*top curve*) and in latitude. The lower two curves are from anticenter direction $b = \pm 10^\circ$ and $45\text{--}60^\circ$ off the plane in latitude (*the halo*). Data points are from: *circles*, Landecker and Wielebinski (1970); *triangles*, Hirabayashi (1974); *squares*, Green (1974). The data at 408 MHz are averages over $\pm 3^\circ$ in latitude at $l = 0^\circ$, $l = 340^\circ$, $l = 20^\circ$ in descending order.

We wish to compare the mean brightness temperature with the locally measured electron intensity. The synchrotron intensities at high frequencies are appropriate, since in a field of $3 \mu\text{gauss}$ a 10 GeV electron has its maximum emission at such frequencies, and because the radio spectral shape at high frequencies agrees with the experimentally measured electron spectral shape with $\gamma = 2.9$.

The experimental data on high-energy electrons are shown in Figure 8, where we have multiplied the differential intensities by $E^{2.7}$. The discrepancies in the data are easily seen in such a plot. Not only do the intensities vary by factors of about 4, but the spectral indices from different observers vary from 2.7 to 3.4. Badhwar, Daniel, and Stephens (1977) have recently commented on these discrepancies and have argued that the radio data with $\alpha = 0.80$ imply that the energy spectrum of radio-emitting electrons in interstellar space must have $\gamma = 2.6$. However, Hirabayashi

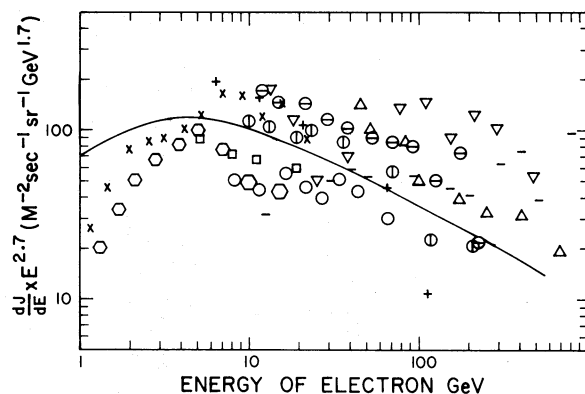


FIG. 8.—Electron differential intensities multiplied by $E^{2.7}$. The line drawn shows intensities predicted from model for lifetime of 10^7 years and $B_{\text{rms}} = 7.5 \mu\text{gauss}$. Data from: *crosses*, Fulks (1975); *hexagons*, Webber and Rockstroh (1973); *open circles*, Freier *et al.* (1977); *dash*, Müller and Meyer (1973); *open square*, Buffington *et al.* (1975); *dagger*, Meegan and Earl (1975); *inverted triangle*, Anand *et al.* (1973); *triangle*, Matsuo *et al.* (1975); *horizontally dashed circle*, Silverberg (1976); *vertically dashed circles*, Hartmann *et al.* (1977). The data have not been corrected for modulation; only below 5 GeV would correction be significant.

(1974) has shown that the spectral index of the radio does steepen to $\alpha = 0.95$ for 3–15 GHz, so that we would expect the electron spectrum to steepen to $\gamma = 2.9$ by 10–20 GeV. Furthermore, electrons of energies of at least 30 GeV will be emitting at frequencies higher than 15 GHz, so there is no direct comparison between them and these radio data.

In Table 2 we compare data from three of the experiments (representing intensity extremes) with the radio data along three different lines of sight: toward center, anticenter, and halo. The radio intensities are those at 3.2 GHz from Figure 7. For these experiments we have calculated K in appropriate units by using γ determined by the authors, and then compared the electrons with the measured radio intensity in different directions to determine the quantity $B^{(\gamma+1)/2}L$. Using line-of-sight distances of 23, 4, and 1 kpc, respectively, for center, anticenter, and halo directions, we obtain values for the mean field of 5–10 μgauss in all directions.

Since we have already allowed a factor of 3 for variations of electron intensity in different regions of the Galaxy, we must inquire how the rms field determined from the radio emission can be a factor of

TABLE 2
PARAMETERS FITTING ELECTRONS TO RADIO DATA

EXPERIMENT	γ	K ergs cm^{-3}	$B^{\gamma+1/2} \mu\text{gauss } L_{\text{kpc}}$			$\bar{B}_{\mu\text{gauss}}$		
			Center	Anticenter	Halo	Center	Anticenter	Halo
Freier <i>et al.</i> (1977)	2.9 ± 0.1	1.9×10^{-17}	2100	227	88	10	8	9
Silverberg (1976)	3.10 ± 0.08	2.4×10^{-17}	960	103	40	6	5	6
Hartmann <i>et al.</i> (1977)	$3.0 - 3.4$	2.4×10^{-17}	1600	171	66	8	6.5	8
$I(3.2 \text{ GHz}) \text{ W m}^{-2} \text{ Hz}^{-1} \text{ Sr}^{-1}$	2.9×10^{-21}	3.1×10^{-22}	1.2×10^{-22}
$L(\text{kpc})$	23	4	1

2 higher than the 3–4 μgauss determined from Faraday rotation and polarization measurements (Heiles 1976). Faraday rotation and polarization measurements vary linearly with B , while synchrotron emission varies as $\sim B^2$. Theoretical considerations (Mouschovias 1976) of the relationships between mass of gas and the B field flux suggest that $B = B_0 n^\kappa$, where $\kappa < 1/2$ and n is the gas density. Suppose that, in the galactic molecular disk (whose height is small compared with its radius), 1% of the volume is filled with clouds with magnetic fields of 100 μgauss , whereas in the intercloud medium with a density of 0.10 cm^{-3} the field is 3.0 μgauss . Then the linear average of B would be 3.5 μgauss , while the rms field is 7.5 μgauss . The clouds and intercloud densities would be 110 and 0.1 atoms cm^{-3} , respectively, giving the required mean density of 1.2 cm^{-3} for the disk. Such matter and field configurations in the disk are thus consistent with magnetic field measurements and radio emission.

Brown and Marscher (1977) have recently considered the synchrotron volume emissivity of such clouds and have concluded that they may be just at the level of detectability as discrete clouds. Including the contribution of such clouds to the radio emission makes it consistent with the locally measured electron intensity. Keep in mind, however, that we have already allowed for a factor of 2–3 for the variation in cosmic-ray electron intensity along different lines of sight.

In Figure 7 the data from the halo are taken toward the anticenter direction at latitudes $b = 45^\circ$ – 60° . The radio emission in this direction, according to our model, will come from a line of sight of $\sim 0.6 \text{ sec } b \sim 1 \text{ kpc}$. An electron intensity equal to that measured locally would require a field of 6–9 μgauss extending to 0.5–1 kpc above the disk. Such bulging magnetic bubbles extending the field from the disk are discussed by Parker (1976).

ii) Electron Lifetime

In addition to the energy-dependent escape, electrons will have their injection spectrum modified by synchrotron and inverse Compton energy-loss effects. Silberberg and Ramaty (1973) have derived the equilibrium spectrum under such conditions

$$N(E) = AE^{-\gamma_0} \int_0^{1/bE} dt (1 - bEt)^{\gamma_0 - 2} \times \exp \left[\frac{-t}{\tau(E)} \left(\frac{1 - (1 - bEt)^{1-\delta}}{bEt(1-\delta)} \right) \right], \quad (7)$$

where the energy-loss rate is $dE/dt = bE^2$ with $b = 10^{-16}(3.8 \times 10^{-2} B^2 + W_\nu)$ $(\text{GeV s})^{-1}$ where B is in μgauss and W_ν is energy density of blackbody and starlight photons. For $W = 0.70 \text{ eV cm}^{-3}$ and $B_{\text{rms}} = 7.5 \mu\text{gauss}$, $b = 2.8 \times 10^{-16} (\text{GeV s})^{-1}$. In Figure 9 we show the results of integration of equation (7) with this value of b and for electron lifetimes varying from 10^6 to 3×10^7 years. For a lifetime of 10^7 years consistent with the nucleon lifetimes, our calculations show that the electrons have a spectral slope varying

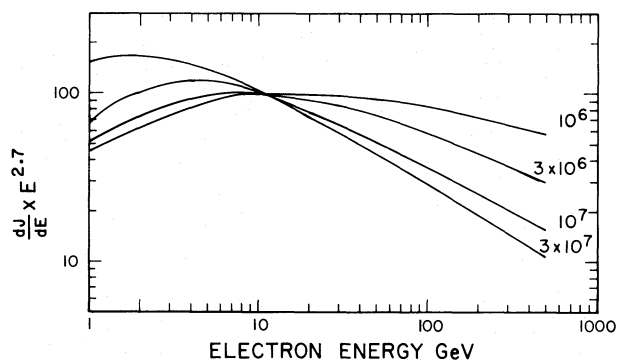


FIG. 9.—Predicted variation of electron intensity (multiplied by $E^{2.7}$) for various lifetimes. The energy loss term $b = 2.8 \times 10^{-16} (\text{GeV s})^{-1}$ commensurable with $B = 7.5 \mu\text{gauss}$.

from the input 2.3 at less than 1 GeV, 2.6 from 3 to 6 GeV, 2.9 from 9 to 15 GeV, 3.1 from 20 to 100, and reaching its asymptotic value of 3.3 at greater than 100 GeV. Except for the relatively flat spectra of Anand, Daniel, and Stephens (1973) with $\gamma = 2.7$ and the Müller and Meyer early results (1973) with $\gamma = 2.66$, the data of various observers do exhibit these slopes, even though there are discrepancies in intensities.

In Figure 8 we have drawn the prediction for a lifetime of 10^7 years. At energies from 1 to 5 GeV this predicted spectrum agrees very well with the limits set from the radio emission (Cummings, Stone, and Vogt 1973). At higher energies the predicted spectrum could agree within a normalization factor with all the data except for the relatively flat spectra mentioned above. We believe that lifetimes greater than 3×10^7 years are ruled out by the limits which can be placed on the demodulated electron intensities, whereas the short lifetimes are not consistent with the steep electron spectra above 10 GeV.

IV. IMPLICATIONS OF THE MODEL

a) Consequences at High Energy

In order to predict the energy spectra for each nuclear species, a full propagation calculation has been carried out. The results are shown in Figures 10 and 11. The equilibrium model for these calculations follows the method of Cowsik and Wilson (1973), which was further described by Hagen (1976) for an exponential path length distribution. The cross sections are computed by using the semiempirical relations of Silberberg and Tsao (1973) which have been updated to account for the latest measurements from the Bevalac (Silberberg *et al.* 1976). Spectra for each component can be found by using Figures 10 and 11 and the iron spectrum from Figure 5. The relative abundances of various nuclei are shown as a function of escape length on the bottom scale. The energy scale along the top is, of course, model-dependent. The source composition is indicated by the asymptotic abundances at high energy (low λ escape).

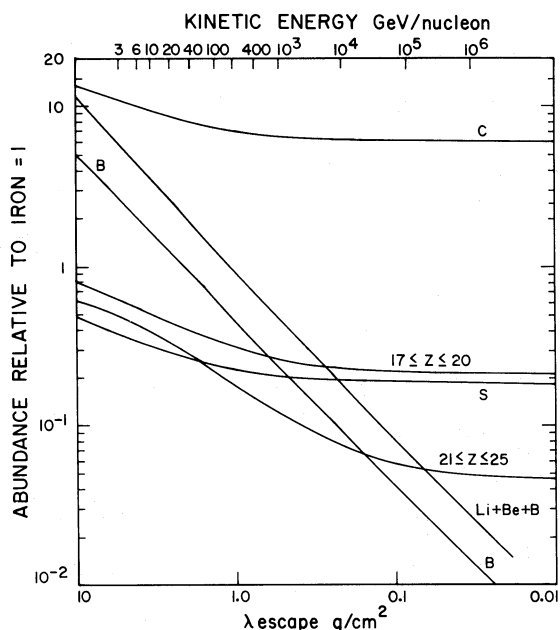


FIG. 10.—Relative abundances normalized to Fe for an exponential distribution in path lengths as a function of the mean escape length using full propagation calculation.

Some of the effects were not apparent from a more simplified approach. The oxygen-to-carbon ratio is predicted to rise about 10% between 3 and 100 GeV per nucleon, whereas the neon-to-carbon ratio should decrease slightly over the same range. The nitrogen spectrum (assumed to be 7.5% of carbon at the source)

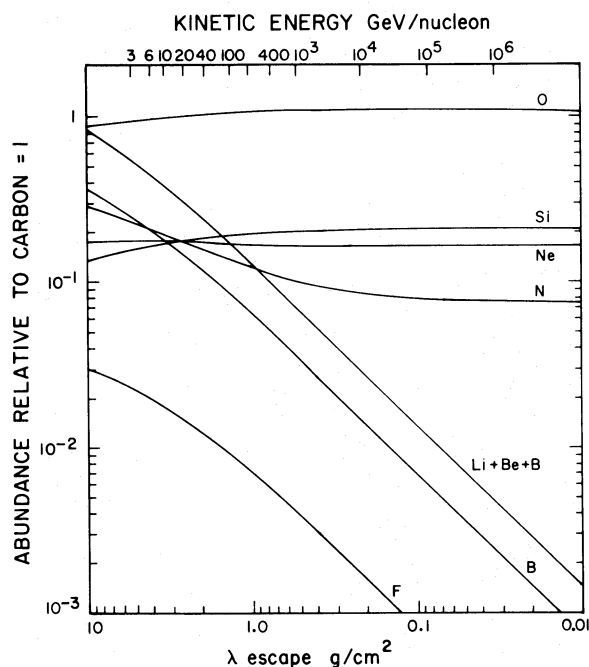


FIG. 11.—Same as Fig. 10 with relative abundances normalized to carbon.

TABLE 3
PREDICTED RELATIVE SPECTRAL INDICES

Observed Component	$\Delta\gamma$	Relative to
B.....	0.31 ± 0.08	C
N.....	0.16 ± 0.04	C
F.....	0.24 ± 0.07	C
C.....	0.11 ± 0.03	Fe
Ne.....	0.12 ± 0.03	Fe
Si.....	0.05 ± 0.01	Fe
$17 \leq Z \leq 20$	0.17 ± 0.04	Fe
$21 \leq Z \leq 25$	0.23 ± 0.06	Fe

is not as steep as are the purely secondary components. From these curves we can estimate the differences in spectral exponent predicted by this model for energies between 3 and 100 GeV per nucleon. The results are given in Table 3. Above 100 GeV per nucleon the composition begins to approach the source composition, but the spectra do not reach their asymptotic values until much higher energies. At all energies the L/M ratio (Li + Be + B/C + N + O) is the most sensitive parameter with which to determine the escape length. The iron secondaries are more sensitive to the distribution in path lengths. The nuclei heavier than iron should most nearly reflect the source spectrum.

At some energy above 100 GeV per nucleon, the wave scattering may become ineffective, and so the escape length (and hence the lifetime) may become short and energy-independent. At these energies spectra of all species should flatten again to the source spectra. This could be what is observed as the flattening of the spectrum at air shower energies (Wdowczyk 1975). Once flattened, the spectra should reflect the source spectrum up to energies where either the acceleration mechanism breaks down (Scott and Chevalier 1975) or galactic confinement becomes improbable.

Whether or not the escape becomes energy-independent, the asymptotic electron spectrum will have $\gamma = \gamma_0 + 1 = 3.3 \pm 0.1$.

There is some evidence that the high-energy iron spectrum, as reflected in the Fe/C + O ratio, Figure 12 (taken from Orth *et al.* 1978), rises faster than predicted in this model. If that should prove true, then a new source of high-energy iron particles would have to be found. A young source ($< 10^6$ years) could enhance the relative abundance of Fe/C + O at high energies (as has been previously suggested by Júlíusson and Meyer 1973).

b) Escape below 7.6 GV

The energy-independent escape length below 7.6 GV rigidity has important consequences. (1) It produces an additional break in the electron spectrum, and at energies below 7.6 GeV the electrons reflect the source spectrum. (2) It causes the spectra of nuclei to flatten to the source spectrum at low energy, thereby reducing the amount of modulation required. (3) It means that the escape time should be inversely proportional to β , making the apparent lifetime longer at low energies.

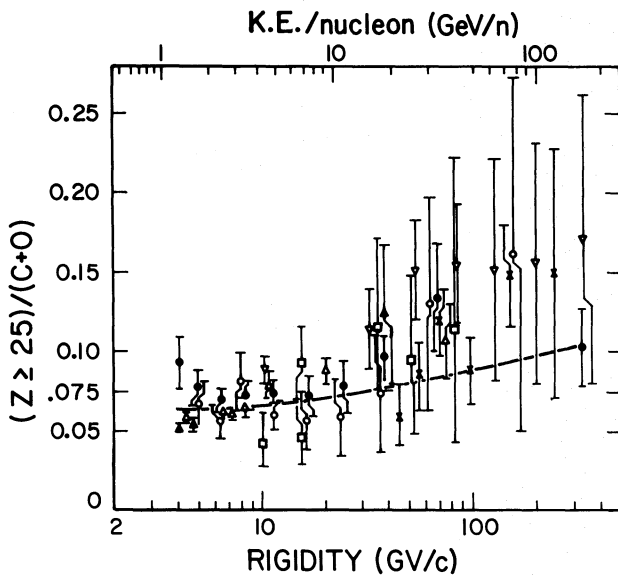


FIG. 12.—The ratio $(Z \geq 25)/(C+O)$ at the top of the atmosphere from Orth *et al.* (1978). The data are from: closed circles, Orth *et al.* (1978); open circles, Smith *et al.* (1973); inverted triangle, Saito *et al.* (1974); crosses, Júlíusson (1974); triangles, Webber, Lezniak, and Kish (1973); square, Ormes and Balasubrahmanyam (1973). The Ormes and Balasubrahmanyam data have been moved down a factor of 2 (Arens and Ormes 1975). The solid line is the prediction of the model.

c) Choice of Source Spectrum

We chose to work with power laws in total energy per nucleon because of the problems of modulating a power law in rigidity. At intermediate energies (1–5 GeV per nucleon) the proton and alpha data exhibit a more constant abundance ratio when expressed in terms of rigidity (Webber and Lezniak 1974). This is an important point which needs further investigation. The source abundance of He will be 15% of protons if spectra are the same in rigidity, but only 4%–5% if spectra are the same in total energy per nucleon.

The Fermi acceleration mechanism (Scott and Chevalier 1975) predicts spectra which are power laws in total energy. Discussions of the acceleration mechanism generally fail to account for the details of scattering which must depend on the rigidity of the particles. Ramadurai and Biswas (1972, 1973) have considered the effects of the velocity dependence, and they present evidence for a spectrum which is intermediate between a power law in total energy per nucleon and rigidity which seems to fit the modulation data. While knowing the appropriate parameter for the source spectrum would reveal important information about the acceleration process, the choice of a source spectrum will not significantly alter the conclusions of this paper.

d) Source Distribution and Energy Requirement

We suggest that the cosmic rays observed at Earth come from sources with an exponential distribution in

distances. The scale length of the sources is 500 pc in the disk, and 50 pc perpendicular to the disk. Particle densities fall off above and below the plane with a scale height of 500 pc or more; if the particles get more than 500 pc above the plane, they have a reduced chance of crossing it again. In fact, the probability of crossing the plane again must fall exponentially with distance from the plane. Wave-scattering theory says that gradients in cosmic-ray intensity perpendicular to the plane are sustained by the waves generated as the particles try to flow down these gradients.

Taking a replacement time of 10^7 years, and a cosmic-ray energy density of 1 eV cm^{-3} as observed near Earth, $\sim 3 \times 10^{52}$ ergs must be supplied per replacement time. Normally the supernova frequency is taken to be 1 SN per 30–100 years. However, a recent radio survey (Clark and Caswell 1976) suggests that this number may be too high currently for our Galaxy and is more like 1 SN per 150 years. In this case there have been 75 SN events in our 1 kpc region in the last 10^7 years. This implies about 5×10^{50} ergs per SN as an energy input. If our region of the Galaxy has a lower-than-average SN rate, this would require a larger energy input; if the lifetime is longer, less energy per event would be required.

e) Path Length Distribution

Owens (1976) has recently examined the age distributions which result from different source distributions. Our model corresponds most closely to his disk model with uniformly distributed sources for which he has derived an almost exponential path length distribution. There is some evidence, based on the secondary nuclei from iron, that low path lengths are underrepresented (see Silberberg and Tsao 1973). This may indicate that we are “outside” the cosmic-ray source, and that all particles must traverse some matter before reaching us.

The experimental evidence suggests that the path length distribution rises from $0\text{--}1 \text{ g cm}^{-2}$ and then falls exponentially above 1 g cm^{-2} . If most particles have passed through 0.5 g cm^{-2} in the interstellar medium, they must be more than 10^6 years old. This may merely reflect the absence of a recent local supernova. This matter could be in the cosmic-ray source itself. It corresponds to a column density of 3×10^{23} atoms cm^{-2} . This is only 30 times the column density of the Cas A source as determined by X-ray observations (Pravdo *et al.* 1976). In the Scott and Chevalier acceleration model the acceleration time is 50–100 years, implying a density of $3\text{--}6 \times 10^3$ atoms cm^{-3} .

f) Local Nature of Cosmic Rays

The model with its “local sphere of influence” provides a natural explanation for the apparently solar-like composition of the cosmic-ray isotopes. Cassé (1977) argues that the abundance distribution of cosmic rays is very similar to the solar composition, provided that the injection abundances are taken inversely proportional to the first ionization potential

of the element. Cassé, in fact, used this to argue that the cosmic rays are local in origin. Hence the isotopic composition of the cosmic rays should be quite like the solar isotopic composition. This is in fact the case (Fisher *et al.* 1976; Dwyer and Meyer 1977), as there are no confirmed observations of nonsolar isotopic composition.

V. CONCLUSIONS

We have shown that the leaky-box model fits both the electron and nuclear data. This is based upon: (1) input spectra varying as $E^{-2.3 \pm 0.1}$, where E is total energy per nucleon (or rigidity), and (2) a rigidity dependent escape $\sim R^{-0.4 \pm 0.1}$ above 7.6 GV and rigidity independent escape = 5.5 g cm^{-2} below 7.6 GV. This is consistent with the cosmic-ray sources being supernova remnants in the disk of the Galaxy. We believe that only sources within 500 pc to 1 kpc contribute significantly to the cosmic rays observed at Earth.

In this leaky-box model, provided the escape length continues to decrease with increasing energy, the spectra of primary nuclei above 100 GeV per nucleon should all approach power laws in total energy with exponent $\gamma_0 + \delta = 2.7$. The purely secondary nuclei should have exponent $\gamma_0 + 2\delta = 3.1$, and the exponent for electrons should be $\gamma_0 + 1 = 3.3$.

Measurements of chemical composition at energies above 100 GeV per nucleon and more accurate measurements between 1 and 100 GeV per nucleon will be important in confirming this model. For example, this model differs substantially from those of Cowsik and Wilson (1973) and Peters and Westergaard (1977) in the predictions of what will happen to the chemical composition at energies greater than 100 GeV per nucleon. In particular, measurements of the spectra of individual secondary components from Si to Ni at high energy will make it possible to determine the source abundances of those nuclei and to check the details of the model.

We have shown how the nuclei and electrons fit this model. The agreement of the γ -ray data to a model which is essentially the same as this has just been shown by Stecker and Jones (1977). They found that the best fit to the γ -ray data is obtained for a cosmic-ray halo of half-thickness 2 ± 2 kpc.

There is still the question of whether or not such a model can explain the isotropy and temporal constancy of the cosmic-ray flux. Extensive measurements on meteorites and lunar rocks have furnished evidence that cosmic rays have been constant within a factor of 2 for 10^9 years, and that the average intensity over the last 400 years is within 10% of that of the last 400,000 years. There is some evidence that the intensity for the most recent 400,000 years is 50% higher than the average for 10^9 years (Schaeffer 1975). In the model there will be an increase in local cosmic rays from a nearby supernova; however, Ramaty (1974) has shown that it will be relatively modest. Such temporal variations can easily be consistent with the not-very-stringent temporal variation data.

The isotropy of cosmic rays provides a more stringent test for the local source model. If the escape length were more strongly dependent on rigidity ($\delta \gg 0.4$), then isotropy might be harder to maintain. There remain the theoretical problems of understanding the exact form of the rigidity dependence of the leakage length, of calculating the effect of the leakage on isotropy, and of understanding the relatively flat ($E^{-2.3}$) input spectrum.

This work was done while one of us (J. F. O.) was a Visiting Professor at the University of Minnesota. He would like to thank the Department and Professor C. J. Waddington for their support and hospitality. We both would like to thank members of the Astronomy Department, particularly Professor John Black, for many helpful discussions, and Dr. V. K. Balasubrahmanyan for his reading of the manuscript. This work was supported by NASA grant 24-005-050.

REFERENCES

- Anand, K. C., Daniel, R. R., and Stephens, S. A. 1973, *Proc. 13th Int. Conf. Cosmic Rays, Denver*, **1**, 335.
 Arens, J. F., and Ormes, J. F. 1975, *Phys. Rev. D.*, **12**, 1920.
 Audouze, J., and Cesarsky, C. 1973, *Nature Phys. Sci.*, **241**, 98.
 Badhwar, G. D., Daniel, R. R., and Stephens, S. A. 1977, *Nature*, **265**, 424.
 Balasubrahmanyan, V. K., and Ormes, J. F. 1973, *A.J.*, **186**, 109.
 Baldwin, J. E. 1976, in *Symposium on The Structure and Content of the Galaxy and Galactic Gamma Rays*, ed. C. E. Fichtel and F. Stecker (Greenbelt: Goddard Space Flight Center), Pub. X-662-76-154, p. 206.
 Brown, R. L., and Marscher, A. P. 1977, *Ap. J.*, **212**, 659.
 Buffington, A., Orth, C. D., and Smoot, G. F. 1975, *Ap. J.*, **199**, 669.
 Burton, W. B. 1976, *Ann. Rev. Astr. Ap.*, **14**, 275.
 Caldwell, J. H. 1977, *Ap. J.*, **218**, 269.
 Cassé, M. 1977, *Bull. Am. Phys. Soc.*, **22**, 643; also thesis l'Université de Paris, 1976.
 Chevalier, R. A., Robertson, J. W., and Scott, J. S. 1976, *Ap. J.*, **207**, 450.
 Clark, D. H., and Caswell, J. L. 1976, *M.N.R.A.S.*, **174**, 267.
 Cowsik, R., and Wilson, L. W. 1973, *Proc. 13th Int. Conf. Cosmic Rays, Denver*, **1**, 500.
 Cummings, A. C., Stone, E. C., and Vogt, R. E. 1973, *Proc. 13th Int. Conf. Cosmic Rays, Denver*, **1**, 335.
 Daniel, R. R., and Stephens, S. A. 1975, *Space Sci. Rev.*, **17**, 45.
 Dwyer, R., and Meyer, P. 1977, *Ap. J.*, **216**, 646.
 Fisher, A. J., Hagen, F. A., Maehl, R. C., Ormes, J. F., and Arens, J. F. 1976, *Ap. J.*, **205**, 938.
 Freier, P. S., Gilman, C., and Waddington, C. J. 1977, *Ap. J.*, **213**, 588.
 Freier, P. S., and Waddington, C. J. 1968, *Phys. Rev.*, **175**, 1641.
 Fulks, G. J. 1975, *J. Geophys. Res.*, **80**, 1701.
 Garcia-Munoz, M., Mason, G. M., and Simpson, J. A. 1975, *Ap. J.*, **202**, 265.
 ———. 1977, *Bull. Am. Phys. Soc.*, **22**, 567.
 Ginzburg, V. L., and Ptuskin, V. S. 1976, *Rev. Mod. Phys.*, **48**, 161.
 Green, A. J. 1974, *Astr. Ap. Suppl.*, **18**, 267.
 Hagen, F. 1976, Ph.D. thesis, University of Maryland.
 Hagen, F. A., Fisher, A. J., and Ormes, J. F. 1977, *Ap. J.*, **212**, 262.

- Hainebach, K. L., Norman, E. B., and Schramm, D. N. 1976, *Ap. J.*, **203**, 245.
- Hartmann, G., Müller, D., and Prince, T. 1977, *Phys. Rev. Letters*, **38**, 1368.
- Heiles, C. 1976, *Ann. Rev. Astr. Ap.*, **14**, 1.
- Hirabayashi, H. 1974, *Pub. Astr. Soc. Japan*, **26**, 263.
- Holmes, J. A. 1975, *M.N.R.A.S.*, **170**, 251.
- Júliusson, E. 1974, *Ap. J.*, **191**, 331.
- Júliusson, E., and Meyer, P. 1973, *Ap. Letters*, **14**, 153.
- Kniffen, D. A., Fichtel, C. E., and Thompson, D. J. 1977, *Ap. J.*, **215**, 765.
- Kulsrud, R. 1975, *Proc. 14th Int. Conf. Cosmic Rays, Munich*, **11**, 3753.
- Kulsrud, R. M., and Cesarsky, C. 1971, *Ap. Letters*, **8**, 189.
- Landecker, T. L., and Wielebinski, R. 1970, *Australian J. Phys. Ap. Suppl.*, No. 16, 1.
- Lezniak, J. A., and Webber, W. R. 1971, *J. Geophys. Res.*, **76**, 1605.
- Lindblad, P. O., Grape, K., Sandqvist, A., and Schaber, J. 1973, *Astr. Ap.*, **24**, 309.
- Lingenfelter, R. E., Ramaty, R., and Fisk, L. A. 1971, *Ap. Letters*, **8**, 93.
- Maehl, R. C., Ormes, J. F., Fisher, A. J., and Hagen, F. A. 1977, *Ap. Space Sci.*, **47**, 163.
- Matsuo, M., Nishimura, J., Kobayashi, T., Niu, K., Aizu, E., Hiraiwa, H., and Taira, T. 1975, *Proc. 14th Int. Conf. Cosmic Rays, Munich*, **12**, 4132.
- McIvor, J. 1977a, *M.N.R.A.S.*, **178**, 85.
- . 1977b, *M.N.R.A.S.*, **179**, 13.
- Meegan, C. A., and Earl, J. A. 1975, *Ap. J.*, **197**, 219.
- Mouschovias, T. 1976, *Ap. J.*, **206**, 753.
- Müller, D., and Meyer, P. 1973, *Ap. J.*, **186**, 841.
- O'Dell, F. W., Shapiro, M. M., Silberberg, R., and Tsao, C. H. 1975, *Proc. 14th Int. Conf. Cosmic Rays, Munich*, **2**, 526.
- Ormes, J. F., and Balasubrahmanyam, V. K. 1973, *Nature Phys. Sci.*, **241**, 95.
- Ormes, J. F., Hagen, F. A., and Maehl, R. C. 1977, private communication.
- Ormes, J. F., and Webber, W. R. 1965, *Proc. 9th Int. Conf. Cosmic Rays, London*, **1**, 407.
- Orth, C. D., Buffington, A., Mast, T. S., and Smoot, G. F. 1978, in press.
- Owens, A. J. 1976, *Ap. Space Sci.*, **40**, 357.
- Owens, A. J., and Jokipii, J. R. 1977, *Ap. J.*, **215**, 677.
- Parker, E. N. 1976, in *Symposium on the Structure and Content of the Galaxy and Galactic Gamma Rays*, ed. C. E. Fichtel and F. Stecker (Greenbelt: Goddard Space Flight Center, pub. X-662-76-154), p. 320.
- Peters, B., and Westergaard, N. J. 1977, in press.
- Pravdo, S. H., Becker, R. H., Boldt, E. A., Holt, S. S., Rothschild, R. E., Serlemitsos, P. J., and Swank, J. H. 1976, *Ap. J. (Letters)*, **206**, L41.
- Puget, J. L., and Stecker, F. W. 1974, *Ap. J.*, **191**, 323.
- Ramadurai, S. 1973, *Ap. Letters*, **14**, 85.
- Ramadurai, S., and Biswas, S. 1972, *Ap. Space Sci.*, **17**, 467.
- Ramaty, R. 1974, in *High Energy Particles and Quanta in Astrophysics*, ed. F. B. McDonald and C. E. Fichtel (Cambridge: MIT Press), p. 122.
- Ramaty, R., Balasubrahmanyam, V. K., and Ormes, J. F. 1973, *Science*, **180**, 731.
- Rasmussen, I. L., and Peters, B. 1975, *Nature*, **258**, 412.
- Reames, D. V. 1974, in *High Energy Particles and Quanta in Astrophysics*, ed. F. B. McDonald and C. E. Fichtel (Cambridge: MIT Press), p. 54.
- Ryan, M. J., Ormes, J. F., and Balasubrahmanyam, V. K. 1972, *Phys. Rev. Letters*, **28**, 985.
- Saito, T., Sato, Y., Sugimoto, H., Matsubayashi, T., and Noma, M. 1974, *J. Phys. Soc. Japan*, **37**, 1462.
- Schaeffer, O. A. 1975, *Proc. 14th Int. Conf. Cosmic Rays, Munich*, **11**, 3508.
- Scott, J. S., and Chevalier, R. A. 1975, *Ap. J. (Letters)*, **197**, L5.
- Setti, G., and Woltjer, L. 1971, *Ap. Letters*, **8**, 125.
- Shapiro, M. M., Silberberg, R., and Tsao, C. H. 1973, *Proc. 13th Int. Conf. Cosmic Rays, Denver*, **1**, 578.
- Shklovskii, I. S. 1960, *Cosmic Radio Waves* (Cambridge: Harvard University Press).
- Silberberg, R., and Tsao, C. H. 1973, *Ap. J. Suppl.*, **25**, 315.
- Silberberg, R., Tsao, C. H., and Shapiro, M. M. 1976, in *Spallation Nuclear Reactions and Their Applications*, ed. B. S. P. Shin and M. Merker (Dordrecht: Reidel), p. 49.
- Silverberg, R. 1976, *Geophys. Res.*, **81**, 3944.
- Silverberg, R. F., and Ramaty, R. 1973, *Nature Phys. Sci.*, **243**, 134.
- Skilling, J. 1975, *Nature*, **258**, 687.
- Smith, L. H., Buffington, A., Smoot, G. F., Alvarez, L. W., and Wahlig, M. A. 1973, *Ap. J.*, **180**, 987.
- Spitzer, L., and Jenkins, E. B. 1975, *Ann. Rev. Astr. Ap.*, **13**, 133.
- Stecker, F. W. 1975, *Phys. Rev. Lett.*, **35**, 188.
- . 1977, *Ap. J.*, **212**, 60.
- Stecker, F. W., and Jones, F. C. 1977, *Ap. J.*, **217**, 843.
- Wdowczyk, J. 1975, *Proc. 14th Int. Conf. Cosmic Rays, Munich*, **11**, 4002.
- Webber, W. R. 1973, *Proc. 13th Int. Conf. Cosmic Rays, Denver*, **5**, 3568.
- . 1976, *Proc. Astr. Soc. Australia*, **3**, 1.
- . 1977, *Bull. Am. Phys. Soc.*, **22**, 555.
- Webber, W. R., and Lezniak, J. A. 1974, *Ap. Space Sci.*, **30**, 361.
- Webber, W. R., Lezniak, J. A., and Kish, J. C. 1973, *Proc. 13th Int. Conf. Cosmic Rays, Denver*, **1**, 248.
- Webber, W. R., Lezniak, J. A., Kish, J. C., and Damle, S. V. 1973, *Nature Phys. Sci.*, **241**, 96.
- Webber, W. R., Lezniak, J. A., Kish, J. C., and Simpson, G. A. 1977, *Ap. Letters*, **18**, 125.
- Webber, W. R., and Ormes, J. F. 1967, *J. Geophys. Res.*, **72**, 5957.
- Webber, W. R., and Rockstroh, J. M. 1973, *J. Geophys. Res.*, **78**, 1.
- Wefel, J. P., Garcia-Munoz, M., Mason, G. M., and Simpson, J. A. 1977, *Bull. Am. Phys. Soc.*, **22**, 567.
- Wentzel, D. G. 1969, *Ap. J.*, **156**, 303.
- . 1974, *Ann. Rev. Astr. Ap.*, **12**, 71.

PHYLLIS FREIER: School of Physics and Astronomy, Tate Laboratory of Physics, University of Minnesota, 116 Church Street, S.E., Minneapolis, MN 55455

JONATHAN ORMES: Code 661, NASA Goddard Space Flight Center, Greenbelt, MD 20771